Molecular Therapy
Methods & Clinical Development
Original Article

Delivery of nVEGFi using AAV8 for the treatment of neovascular age-related macular degeneration

Kaiqin She,[1,2] Jing Su,[2] Qingnan Wang,[2,3] Yi Liu,[2] Xiaomei Zhong,[2] Xiu Jin,[2] Qinyu Zhao,[2] Jianlu Xiao,[2] Ruiting Li,[2] Hongxin Deng,[2] Fang Lu,[1] Yang Yang,[2] and Yuquan Wei[2]

[1]Department of Ophthalmology, West China Hospital, Sichuan University, No.37, Guoxue Xiang, Chengdu, Sichuan 610041, China; [2]State Key Laboratory of Biotherapy and Cancer Center, West China Hospital, Sichuan University and Collaborative Innovation Center, No. 1, Ke-yuan Road 4, Gao-peng Street, Chengdu, Sichuan 610041, China

Inhibition of vascular endothelial growth factor (VEGF) is the standard therapy for neovascular age-related macular degeneration (nAMD). However, anti-VEGF agents used in the clinic require repeated injections, causing adverse effects. Gene therapy could provide sustained anti-VEGF levels after a single injection, thereby drastically decreasing the treatment burden and improving visual outcomes. In this study, we developed a novel VEGF Trap, nVEGFi, containing domains 1 and 2 of VEGFR1 and domain 3 of VEGFR2 fused to the Fc portion of human IgG. The nVEGFi had a higher expression level than aflibercept under the same expression cassettes of adeno-associated virus (AAV)8 *in vitro* and *in vivo*. nVEGFi was found to be noninferior to aflibercept in binding and blocking VEGF *in vitro*. AAV8-mediated expression of nVEGFi was maintained for at least 12 weeks by subretinal delivery in C57BL/6J mice. In a mouse laser-induced choroidal neovascularization (CNV) model, 4×10^8 genome copies of AAV8-nVEGFi exhibited a significantly increased reduction in the CNV area compared with AAV8-aflibercept (78.1% vs. 63.9%, $p < 0.05$), while causing no structural or functional changes to the retina. In conclusion, this preclinical study showed that subretinal injection of AAV8-nVEGFi was long lasting, well tolerated, and effective for nAMD treatment, supporting future translation to the clinic.

INTRODUCTION

Age-related macular degeneration (AMD) is a progressive macular disease. Late-stage AMD results in severe and permanent central vision impairment and legal blindness, which has an impact on quality of life. Neovascular AMD (nAMD) and atrophic AMD are two types of late-stage AMD.[1] Because of the exponential population aging globally, the projected number of people with AMD in 2020 is 196 million, increasing to 288 million in 2040,[2] thus posing a major public health issue with significant socioeconomic ramifications.

Neovascular AMD is characterized by choroidal neovascularization (CNV), incorporating with exudation, intraretinal and subretinal hemorrhage, retinal pigment epithelial detachment, hard exudate, or subretinal fibrous scar.[1] Vascular endothelial growth factor (VEGF) is a major mediator in angiogenesis and CNV formation.[3] The advent of anti-VEGF molecules drastically changed the treatment of nAMD, before which laser photocoagulation and photodynamic therapy with verteporfin were used.[4,5] The intravitreal injection of anti-VEGF molecules demonstrates successful prevention of severe visual loss and is the current standard care for patients with nAMD. However, the widely used anti-VEGF agents in the clinic, including bevacizumab, ranibizumab, aflibercept, conbercept, and brolucizumab have short half-lives, thus requiring repeated injections, which can cause intraocular inflammation, retinal detachment, and ocular hemorrhage.[6] Meanwhile, in the real world, patients receive insufficient injections and visits, resulting in a lower visual acuity gain than in phase III clinical trials.[7] Gene therapy can solve this problem by two major strategies based on intraocular delivery of viral vector encoding antiangiogenic proteins or noncoding RNA interference targeting overexpression of VEGF, which gives a lifelong continuous supply of antiangiogenic proteins or small interfering RNA by a single injection, dramatically reducing injection frequency.[8–13]

Antiangiogenic proteins, including pigment epithelium-derived factor, endostatin, and angiostatin, and anti-VEGF proteins, such as soluble fms-like tyrosine kinase-1, aflibercept, and ranibizumab, have been assessed for potential gene therapy for nAMD in clinical trials.[14–16] Among them, aflibercept and ranibizumab delivered by adeno-associated virus (AAV) vectors showed optimistic results in reducing injection frequencies in clinical trials for nAMD treatment (ADVM-022: AAV2.7m8-aflibercept, NCT03748784; RGX-314: AAV8-ranibizumab, NCT03066258).[8,9] However, it is noteworthy that the high rescue injection-free rate is relevant to a high dose of AAV, that is 12 out of 16 patients at 6×10^{11} genome copies (GC) and 8 out of 15 patients at 2×10^{11} GC with ADVM-022, 9 out of 12 patients at 2.5×10^{11} GC, and 5 out of 12 patients at 1.6×10^{11}

Received 2 August 2021; accepted 5 January 2022;
https://doi.org/10.1016/j.omtm.2022.01.002.

[3]Present address: Chengdu Genevector Therapeutics Inc., Chengdu, China

Correspondence: Department of Ophthalmology, West China Hospital, Sichuan University, No.37, Guoxue Xiang, Chengdu, Sichuan 610041, China.
E-mail: lufang@wchscu.cn
Correspondence: State Key Laboratory of Biotherapy and Cancer Center, West China Hospital, Sichuan University and Collaborative Innovation Center, No. 1, Ke-yuan Road 4, Gao-peng Street, Chengdu, Sichuan 610041, China.
E-mail: yang2012@scu.edu.cn

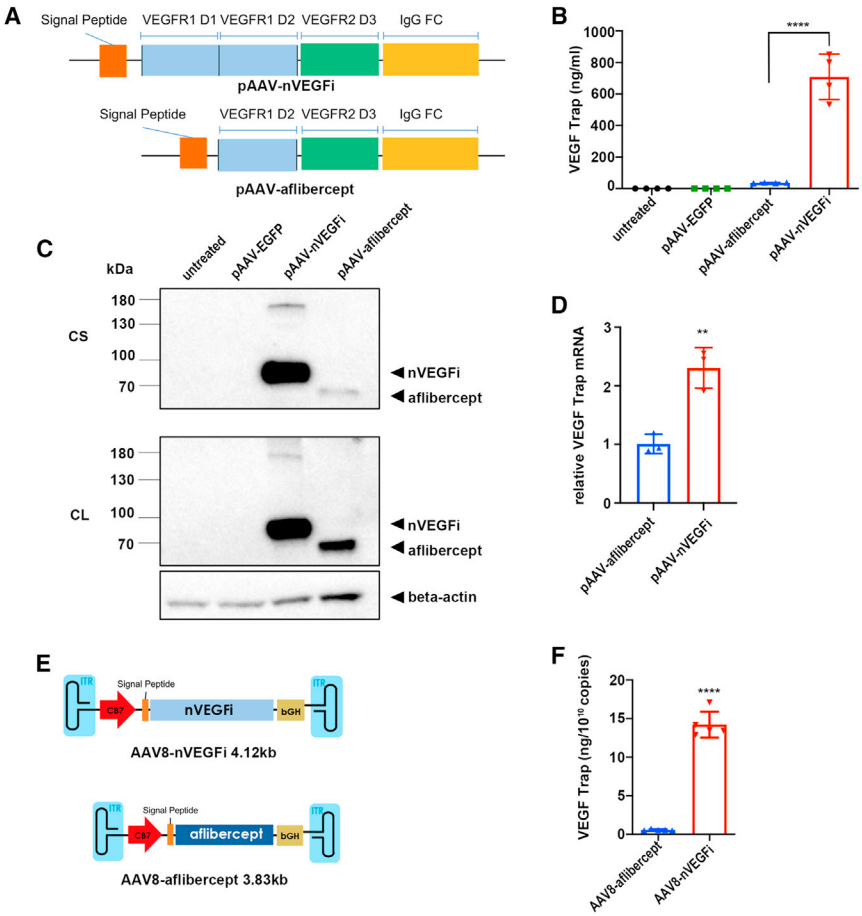

Figure 1. Higher expression level of nVEGFi *in vitro*

(A) Schematic of the encoding sequence of the plasmid expressing nVEGFi (upper) and the plasmid expressing aflibercept (below). (B) ELISA of VEGF Traps in HEK293 cell supernatant transfected with pAAV-EGFP, pAAV-aflibercept or pAAV-nVEGFi at equal molar. Data are expressed as the mean ± SD (n = 4). Student's *t* test for comparison between pAAV-aflibercept and pAAV-nVEGFi treated groups: ****p < 0.0001. (C) Western blot analysis of VEGF Traps in the HEK293 cell supernatant (CS) and cell lysates (CL) transfected with pAAV-EGFP, pAAV-aflibercept, or pAAV-nVEGFi at equal molar. (D) Relative VEGF Trap mRNA expression in cells transfected with equal molar pAAV-aflibercept or pAAV-nVEGFi was measured by real-time qPCR and normalized to beta-actin and compared to pAAV-aflibercept. Data are expressed as mean ± SD (n = 3). Student's *t* test: **p < 0.01. (E) Schematic presentations of the AAV8-nVEGFi vector (upper) and AAV8-aflibercept vector (below). The AAV vectors contain the CB7 promotor, a chicken β-actin intron, a kozak sequence, the signal peptide, nVEGFi, or aflibercept transgene and bGH polyadenylation sequence flanked by AAV2 ITRs. (F) ELISA of VEGF Traps in HEK293 cell supernatant infected with AAV8-aflibercept or AAV8-nVEGFi at equal MOI. Data are expressed as the mean ± SD (n = 5). Student's *t* test: ****p < 0.0001

GC with RGX-314. However, a higher virus dose means a higher incidence of intraocular inflammation.[17,18] In addition, a high dose of ADVM-022 (6×10^{11} GC/eye) showed toxicity when evaluated in patients with diabetic macular edema.[19]

All these findings highlight the importance of optimizing the anti-VEGF vector by enhancing the expression of the anti-VEGF molecule to reduce the effective dose of virus and to reduce toxicity and immunogenicity. We designed a novel VEGF Trap, nVEGFi, containing domains 1 and 2 of VEGF receptor 1 and domain 3 of VEGF receptor 2 fused to the Fc portion of human IgG to enhance the protein expression level without compromising its anti-VEGF efficacy. AAV is the most popular vector system for ocular gene therapy because of its nonintegrating nature, low immunogenicity, and potential long-term gene expression.[20] When delivered subretinally, AAV8 demonstrated strong transduction of both RPE and photoreceptors.[21] The use of AAV8 vectors to express nVEGFi may help to maximize long-term suppression of VEGF in the eye and overcome limitations of past gene transfer approaches in nAMD. In this study, we used a mouse laser-induced CNV model to test the efficacy of subretinal injection in a wide range of doses of an AAV8 vector containing an expression cassette for nVEGFi.

RESULTS

Novel nVEGFi provided a higher expression level *in vitro*

Aflibercept is a VEGF Trap comprising the second Ig domain of human VEGFR1 and the third Ig domain of human VEGFR2 expressed as an inline fusion with the Fc portion of human IgG, which binds to VEGF-A, VEGF-B, and placental growth factor (PlGF) and inhibits the activation of VEGFR1 and VEGFR2.[22] We designed a novel VEGF Trap, named nVEGFi, containing the first and second Ig domains of human VEGFR1 as well as the third Ig domain of human VEGFR2 linked to the human IgG Fc region that resulted in the formation of a forced homodimer (Figure S1). nVEGFi had an identical sequence to aflibercept except for the addition of VEGFR1 Ig domain 1 in the N-terminus. The AAV *cis* plasmid pAAV-nVEGFi was then constructed to express nVEGFi (Figure 1A, upper). Meanwhile, pAAV-aflibercept-expressing aflibercept was constructed with the same other expression cassettes as pAAV-nVEGFi (Figure 1A, below). pAAV-EGFP serves as a negative control expressing EGFP. All three plasmids were under the control of a CB7 promoter and used for transfection of HEK293 cells at equimolar doses. ELISA showed that the concentration of VEGF Trap (ng/mL) in the cell supernatant transfected with pAAV-nVEGFi was 19.3 times higher than that transfected with pAAV-aflibercept (mean ± SD, pAAV-nVEGFi 709.0 ± 144.0 ng/mL, pAAV-aflibercept 36.7 ± 1.6 ng/mL) (Figure 1B). The VEGF Trap in cell supernatant and lysates was detected by western blot, demonstrating that the amount of VEGF Trap in cell supernatant transfected with pAAV-nVEGFi is around

Table 1. Kinetic binding parameters for nVEGFi and aflibercept binding to human VEGF family ligands determined by SPR-Biacore

VEGF inhibitor	Ligand	Kinetic binding parameters		
		ka/10^5 (M^{-1} s^{-1})	kd/10^3 (s^{-1})	KD (pM)
nVEGFi	VEGF-A_{165}	46.6	12.6	27.1
	PlGF	6.19	78.4	1270
Aflibercept	VEGF-A_{165}	116	17	14.7
	PlGF	8.11	1.41	1740

16-fold higher than that of pAAV-aflibercept, and approximately 4 times in cell lysates normalized by beta-actin (Figure 1C). Next, relative nVEGFi mRNA or aflibercept mRNA in transfected cells was measured, and it turned out that the transcription level of nVEGFi was 2.3 times higher than that of aflibercept ($p < 0.01$) (Figure 1D). All these findings indicated that the addition of VEGFR1 domain 1 can increase the mRNA and protein expression levels of VEGF Trap and, more importantly, can increase the secretion of VEGF Trap.

Then, the nVEGFi and aflibercept expression cassettes were packaged into AAV8, with a strong CB7 promoter, a chicken β-actin intron, a kozak sequence, and a bGH polyadenylation sequence (Figure 1E). Except for the inclusion of VEGFR1 Ig domain 1, AAV8-nVEGFi had the same sequences as AAV8-aflibercept. Next, AAV8-nVEGFi and AAV8-aflibercept were used to transduce HEK293 cells with the help of adenovirus under the same conditions. ELISA showed that the level of VEGF Trap (ng/10^{10} copies) in the cell supernatant transduced with AAV8-nVEGFi was 25.8 times higher than that transduced with AAV8-aflibercept (mean ± SD, AAV8-nVEGFi 14.21 ± 1.68 ng/10^{10} copies, AAV8-aflibercept 0.55 ± 0.09 ng/10^{10} copies) (Figure 1F).

nVEGFi exhibited noninferior binding affinity and inhibition property to aflibercept *in vitro*

Since the addition of VEGFR1 domain 1 could significantly enhance the protein expression level, we next compared nVEGFi to aflibercept for their ability to bind and block VEGF *in vitro*. We first synthesized and purified nVEGFi protein. The binding affinity of nVEGFi for VEGF family ligands, including VEGF-A_{165} and PlGF, was measured with SPR-Biacore technology. Similar to aflibercept, nVEGFi can target VEGF-A_{165} and PlGF (Table 1). Meanwhile, the binding affinity was also measured by equilibrium binding assay, in which different concentrations of nVEGFi or aflibercept were incubated with VEGF-A_{165}, and the amount of free VEGF-A_{165} was measured, demonstrating that nVEGFi had a similar VEGF-binding affinity to aflibercept (Figure 2A).

Next, the ability to block VEGF-stimulated human umbilical vein endothelial cell (HUVEC) proliferation was assessed by MTS assay for the nVEGFi protein and cell supernatant of pAAV-nVEGFi-transfected cells, with aflibercept as a control. In agreement with the VEGF-binding affinity assay, all of them demonstrated an equal inhibitory effect on VEGF-dependent HUVEC proliferation (Figure 2B).

In vivo dose-escalation efficacy study of AAV8-nVEGFi in comparison with AAV8-aflibercept

According to the above studies, nVEGFi was at least as effective as aflibercept as a VEGF blocker and had a significantly higher expression level, which made it more suitable for gene therapy. First, an *in vivo* dose-escalation efficacy study of AAV8-nVEGFi was carried out, in which 4-week-old C57BL/6J mice were subretinally injected with AAV8-nVEGFi at 4×10^6, 4×10^7, 4×10^8 or 4×10^9 GC/eye or PBS (vehicle of AAV or proteins) as a vehicle control. Retinal laser photocoagulation was performed 4 weeks post injection to induce CNV (see Figure 3A for an illustration of AAV treatment timelines and a typical fundus image with an injection bleb). In addition, we established aflibercept and nVEGFi protein treated groups. In these two groups, mice were intravitreally injected with 2.5 μg/eye aflibercept or an equimolar dose of nVEGFi on the same day as the laser at 8 weeks old.

Six days after laser photocoagulation, fundus fluorescein angiography (FFA) showed decreased leakage in AAV8-nVEGFi at 4×10^8 and 4×10^9 GC/eye, as well as aflibercept and nVEGFi protein treated groups (representative pictures in Figure 3B). The retinal pigment epithelium (RPE)-choroid-sclera complexes were prepared for Isolectin-B4 (IB4) staining and evaluation of the CNV area 7 days after laser photocoagulation. The CNV area was significantly reduced in groups treated with subretinal injection of AAV8-nVEGFi at 4×10^8 (−78.1%, $p < 0.0001$) and 4×10^9 (−80.4%, $p < 0.0001$) GC/eye and in groups treated with intravitreal injection of aflibercept (−79.7%, $p < 0.0001$) and nVEGFi protein (−77.3%, $p < 0.0001$) compared to PBS control group, with no significant difference among these four groups (Figures 3C and 3D). These results demonstrated that intravitreal injection of nVEGFi protein and subretinal injection of AAV8-nVEGFi at 4×10^8 and 4×10^9 GC/eye had the same anti-VEGF ability as aflibercept *in vivo*.

To compare AAV8-nVEGFi to AAV8-aflibercept, mice were injected with AAV8-aflibercept at 4×10^8 or 4×10^9 GC/eye and treated with the same procedure as before (Figure 3A). FFA showed that AAV8-aflibercept at both doses reduced leakage (Figure 3B). Compared to the PBS-treated group, the CNV area was reduced 63.9% at 4×10^8 GC/eye ($p < 0.0001$) and 67.8% at 4×10^9 GC/eye ($p < 0.0001$) (Figures 3C and 3D). However, the reduction was significantly decreased compared with AAV8-nVEGFi at the same dose, 4×10^8 GC/eye ($p < 0.05$) or 4×10^9 GC/eye ($p < 0.05$).

Long-term expression of AAV8-nVEGFi *in vivo*

To compare the expression of AAV8-nVEGFi and AAV8-aflibercept *in vivo*, AAV8-nVEGFi vector at 4×10^6, 4×10^7, 4×10^8, or 4×10^9 GC/eye, or AAV8-aflibercept vector at 4×10^8 or 4×10^9 GC/eye were administered by subretinal injection to 4-week-old C57BL/6J mice, with PBS as a negative control. Since the expression of AAV8-nVEGFi was stable from 4 weeks to 12 weeks post injection

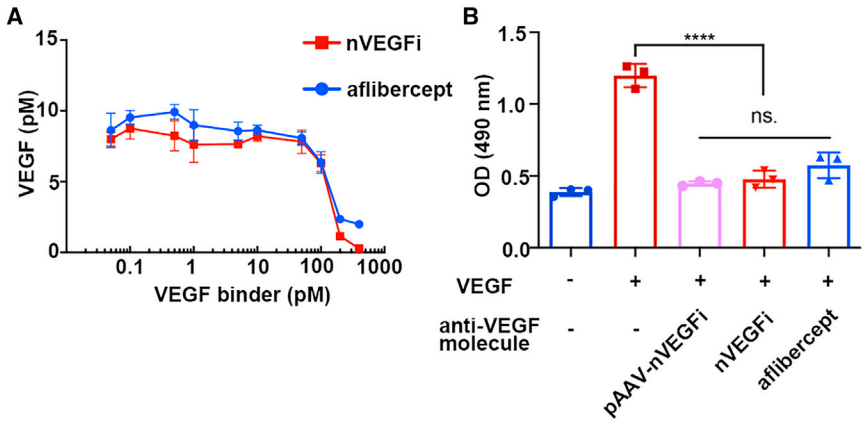

Figure 2. Comparison of the binding affinity and inhibition property of nVEGFi to aflibercept

(A) VEGF binding affinities of nVEGFi and aflibercept, measured by equilibrium binding assay, in which the amount of free VEGF-A_{165} was measured after incubation of 10 pM VEGF-A_{165} with different concentrations of nVEGFi or aflibercept. Data are expressed as the mean ± SD (n = 2). (B) Inhibitory effect of the supernatant of pAAV-nVEFGi transfected cells, nVEGFi protein, and aflibercept on VEGF-induced HUVEC proliferation, measured by MTS assay. The final concentration of anti-VEGF molecules was 1,100 pM. Specifically, the concentration of nVEGFi in the cell supernatant of pAAV-nVEGFi was measured by ELISA. Data are expressed as mean ± SD (n = 3). One-way ANOVA with Tukey's *post hoc* test; difference between 'VEGF + anti-VEGF molecule -' and anti-VEGF molecules, ****$p < 0.0001$, ns. not significant difference.

(Figure S2), the eyes were enucleated for VEGF Trap expression levels measured by ELISA at 12 weeks post injection. The nVEGFi protein expression in AAV8-nVEGFi treated groups showed a dose-dependent increase, with 14.06 ± 11.74 ng/eye in the 4×10^6 GC dosing group (n = 10), 332.8 ± 227.8 ng/eye in the 4×10^7 GC dosing group (n = 9), 3503 ± 856.9 ng/eye in the 4×10^8 GC dosing group (n = 8), and 4132 ± 1215 ng/eye in the 4×10^9 GC dosing group (n = 9) (Figure 4A). The aflibercept protein expression in the AAV8-aflibercept treated groups was 640.8 ± 154.1 ng/eye in the 4×10^8 GC dosing group (n = 10) and 1309 ± 695.6 ng/eye in the 4×10^9 GC dosing group (n = 10). The protein expression in AAV8-nVEGFi treated group is significantly higher than AAV8-aflibercept treated group at the same dose, that is approximately 5.5 times higher in 4×10^8 GC dosing group ($p < 0.0001$) and approximately 3.2 times higher in 4×10^9 GC dosing group ($p < 0.0001$).

In situ hybridization was used to detect nVEGFi mRNA in the retinas of AAV8-nVEGFi-treated mice 12 weeks post injection. The number of transduced retinal cells increased with increasing vector dose (Figures 4B–4F). No specific staining of the retina was observed in PBS treated eyes (Figures 4B and 4B′). The 4×10^6 CG/eye group showed staining only in RPE cells (Figures 4C and 4C′). The 4×10^7 GC/eye group showed staining mainly in RPE cells and the inner segment/out segment (IS/OS) layer, with scattered fluorescence in the outer nuclear layer (ONL), outer plexiform layer (OPL), and inner nuclear layer (INL) (Figures 4D and 4D′). The 4×10^8 GC/eye group showed staining in the RPE, IS/OS layer, ONL, OPL, INL, and inner plexiform layer (Figures 4E and 4E′). The 4×10^9 GC/eye group showed a much more extensive staining in the RPE and the whole retina layers, including the ganglion cell layer. In addition, retinal sections of 4×10^6, 4×10^7, and 4×10^8 GC/eye treated eyes were stained locally, and 4×10^9 GC/eye showed extensive staining of the whole retina and obvious segmental retinal degeneration, which was proposed to be related to the toxicity of the high dose of vector (Figures 4F and 4F′). The extent of the transduction depends on the injection itself, but the dose of AAV will affect the transduced portion in the injection area.

Safety of AAV8-nVEGFi in C57BL/6J mice at different doses

To evaluate the potential toxicity of AAV8-nVEGFi to the retina, PBS and AAV8-nVEGFi from 4×10^6 to 4×10^9 GC/eye were delivered subretinally to C57BL/6J male mice at 4 weeks of age. Meanwhile, AAV8-aflibercept or AAV8-EGFP at 4×10^8 or 4×10^9 GC/eye was injected as a control. Subsequently, full-field scotopic electroretinography (ERG) was performed at 4 weeks and 12 weeks after the injection, and mice were sacrificed for light microscopy evaluation immediately after the second ERG analysis.

We found a significant dose-related decrease in ERG amplitudes in eyes treated with AAV8-nVEGFi, AAV8-aflibercept, and AAV8-EGFP. Eyes injected with AAV8-nVEGFi at the higher dose (4×10^9 GC/eye) resulted in a decrease in both b-wave (−52.8%, $p < 0.001$) and a-wave amplitudes (−34.6%, $p > 0.05$) at 4 weeks post injection. The decrease in ERG was more pronounced at 12 weeks post injection, with a 60.1% ($p < 0.01$) decrease in b-wave amplitude and a 70.1% ($p < 0.0001$) decrease in a-wave amplitude. Eyes injected with AAV8-nVEGFi at 4×10^6, 4×10^7 or 4×10^8 GC/eye showed no deterioration in ERG (Figure 5A). However, eyes treated with AAV8-aflibercept and AAV8-EGFP revealed a deteriorated ERG at both 4×10^8 and 4×10^9 GC/eye, with b-wave amplitude decreased by 66.4% in AAV8-aflibercept at 4×10^8 GC/eye, 83.0% in AAV8-aflibercept at 4×10^9 GC/eye, 85.5% in AAV8-EGFP at 4×10^8 GC/eye and 96.6% in AAV8-EGFP at 4×10^9 GC/eye 12 weeks post injection (Figure 5A).

Consistently, no significant retinal tissue abnormality was found in eyes treated with 4×10^6, 4×10^7, or 4×10^8 GC/eye AAV8-nVEGFi compared to PBS (Figures 5B and S3). However, eyes treated with 4×10^9 GC/eye presented with locally extensive ONL thinning, which was also present in eyes treated with AAV-aflibercept at 4×10^9 GC/eye and AAV-EGFP at 4×10^8 and 4×10^9 GC/eye (Figures 5B and S4). In summary, dose levels of AAV8-nVEGFi from 4×10^6 to 4×10^8 GC/eye GC/eye were well tolerated. AAV8-nVEGFi at 4×10^9 GC/eye, AAV8-aflibercept and AAV-EGFP at 4×10^8 and 4×10^9 GC/eye were associated with progressive reductions in ERG signals and retinal atrophy.

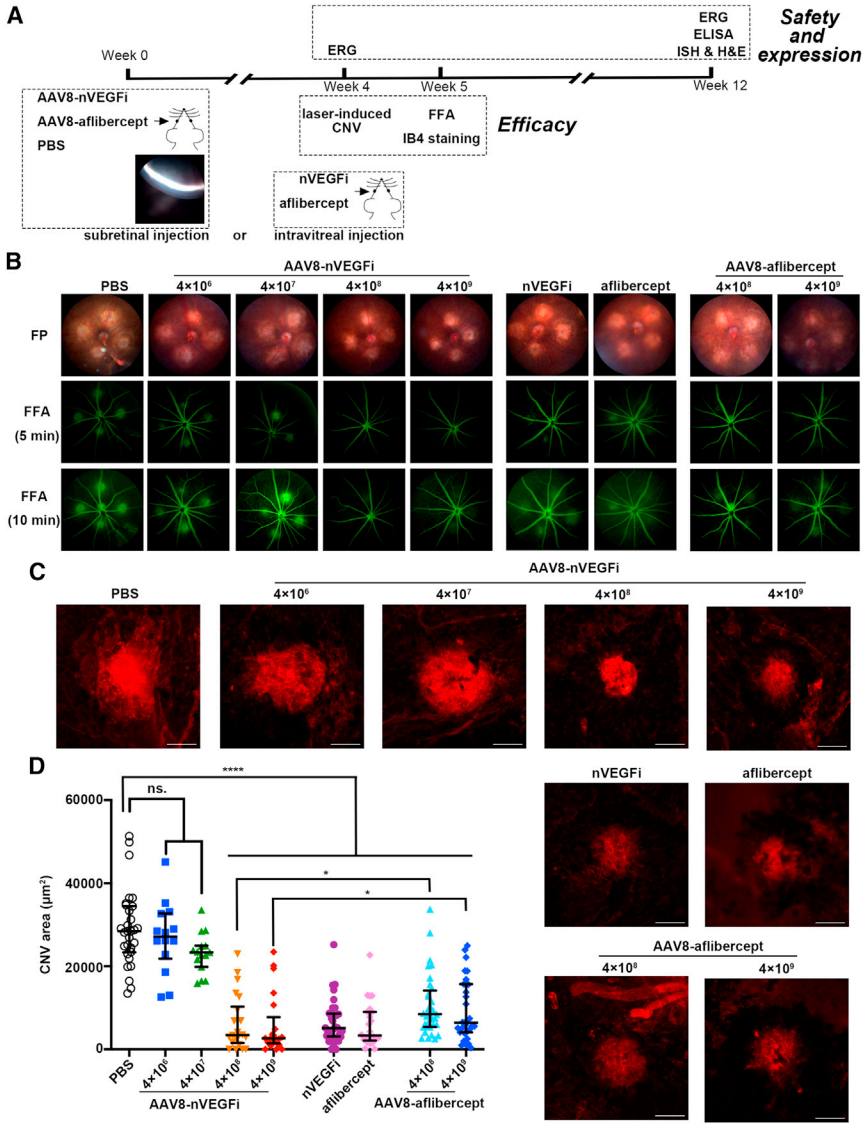

Figure 3. CNV inhibition of AAV8-nVEGFi

(A) Study design and timeline of the experimental setup used to assess the *in vivo* efficacy, safety, and expression of AAV8-nVEGFi. Mice were subretinally injected with 1 μL PBS, AAV8-nVEGFi at 4×10^6, 4×10^7, 4×10^8, or 4×10^9 GC/eye, or AAV8-aflibercept at 4×10^8 or 4×10^9 GC/eye at 4 weeks of age. For the efficacy study, 4 weeks after injection, mice were treated with laser photocoagulation. For the aflibercept and nVEGFi protein treated groups, mice were intravitreally injected with 2.5 μg/eye aflibercept or an equimolar dose of nVEGFi protein immediately after laser treatment at 8 weeks of age. More than 8 eyes were used in each group. Six days after laser, FFA was performed. Seven days after laser photocoagulation, RPE-choroid-sclera complexes were prepared for IB4 staining and evaluation of the CNV area. For safety and expression studies, mice did not receive laser photocoagulation. ERG was performed 4 and 12 weeks after injection, and eyes were collected for expression and histology studies 12 weeks after injection. (B) Representative fundus photographs (FP) and FFA taken 5 and 10 min after fluorescein injection for mice at 6 days after laser photocoagulation. (C) Representative CNV staining with IB4 in mouse eyes 7 days after laser photocoagulation. Scale bars, 75 μm. (D) The CNV area. Data are expressed as the median (Q25, Q75), n > 13 burns for each group. Differences among multiple groups were examined by the Kruskal-Wallis test with *post hoc* Dunnett's test: ****p < 0.0001 L; *p < 0.05; ns. nonsignificant difference.

DISCUSSION

This study describes a novel VEGF Trap, nVEGFi, with comparable anti-VEGF efficacy to aflibercept. However, the addition of the first domain of VEGFR1 in nVEGFi resulted in a significantly higher amount of expression than aflibercept under the same conditions *in vitro* and *in vivo*. Because nVEGFi and aflibercept are secretory proteins that work extracellularly, the amount of VEGF Traps was first measured in the supernatant of cells transfected with plasmids or infected with AAV. When cells were transfected with plasmids, the amount of nVEGFi in the supernatant was 19.3 times higher than aflibercept, and when cells were infected with AAV with plasmids, it was 25.8 times higher. The expression of nVEGFi in cells *in vitro* was approximately 2.3 times higher at the mRNA level and nearly 4 times higher at the protein level than aflibercept. The expression of AAV8-nVEGFi *in vivo* was approximately 5.5 times higher than that of AAV8-aflibercept at 4×10^8 GC/eye, consistent with the *in vitro* results. The comparison of the expression level of VEGF Traps by the amounts of proteins, even transfected with the equal molar of plasmids or same copies of virus, is complicated by the different molecular weights of the two VEGF Traps. Aflibercept is a dimeric glycoprotein with a protein molecular weight of 97 kDa and contains glycosylation, constituting an additional 15% of the total molecular mass, resulting in a total molecular weight of 115 kDa. nVEGFi is also a dimeric protein with a protein molecular weight of approximately 125 kDa, which is approximately 1.3 times that of aflibercept. Even when the greater molecular weight is taken into consideration, adding domain 1 of VEGFR1 can boost the expression and, more predominantly, secretion of VEGF Trap. However, it is unknown why expression and secretion have improved.

The nVEGFi was designed based on the extracellular domains of VEGFR1, which have a higher VEGF-A binding affinity than VEGFR2 and can also bind to VEGF-B and PlGF.[23] The second domain of VEGFR1 contains critical determinates required for the interaction with VEGF and PlGF, but full binding requires the additional presence of flanking domains 1 and 3, which can

be substituted by the homologous domains of other VEGF receptors.[24,25] Holash et al.[22] reengineered VEGF-Traps and found that aflibercept, containing VEGFR1 domain 2 and VEGFR2 domain 3, was one of the most potent and effective VEGF blockers among a group of VEGF Traps because of its improved pharmacokinetic profile and high binding affinity to VEGF.[22] VEGF-Grab, containing the second and third domains of VEGFR1 fused to human IgG1 Fc, was developed with stronger antiangiogenic efficacy than aflibercept.[26] We designed nVEGFi, consisting of domains 1 and 2 of VEGFR1 and domain 3 of VEGFR2, and found that it had a higher expression and noninferior VEGF binding affinity and inhibition properties than aflibercept. Even though no pharmacokinetic evaluation was performed, the intravitreal injection of nVEGFi showed a similar CNV inhibition to aflibercept at the equimolar dose, which indicated that nVEGFi could be another potential anti-VEGF agent.

AAV8 was chosen to deliver nVEGFi because of its strong transduction of both RPE and photoreceptors.[21] According to the fluorescence *in situ* hybridization results, the RPE is the first transduced cell at the lower dose of AAV8-nVEGFi. The whole retina could be transduced at a higher dose, which is in line with a previous study.[21] Both retinal cell-type-specific promoters and ubiquitous promoters have been employed in gene therapy of ocular diseases.[27] In most clinical trials of gene therapy for nAMD, ubiquitous promoters, including CB7/CAG, CMV and CAG, were used, which can drive much higher gene expression than many tissue-specific promoters.[18,28,29] Tissue-specific expression has also been evaluated in mice to express miRNAs or proteins in specific cells, usually RPE, to downregulate angiogenesis to treat nAMD.[30–32] In addition, inducible regulation of transgene expression could be a promising approach for regulating anti-VEGF agent dose to fit the patient-specific effective dose.[31,33] Despite gene augmentation or gene silencing, gene knockout by the CRISPR/Cas system showed the potential to ablate pathologic angiogenesis and treat nAMD.[34–37]

The two most common ways to deliver AAV are intravitreal and subretinal injections. Subretinal injection leads to superior retinal gene transfer compared with intravitreal injection in nonhuman primates.[38,39] Moreover, intravitreal injection causes increased and persistent distribution of vector genomes in blood and lymphatic tissues, raising concerns regarding the immune response and off-target transduction.[38,40] In this case, subretinal injection of AAV8-nVEGFi was used in this study. Currently, subretinal injection involves vitrectomy surgery, which is subject to potential complications.[41] A novel method of subretinal injections using transscleral microneedles eliminates the need for vitreoretinal surgery, simplifying the procedure and reducing the risks associated with the procedure,[42] which could be considered for further experiments in nonhuman primates and clinical trials. Suprachoroidal injection could provide widespread transgene expression in the RPE but might lead to localized inflammation in rhesus macaques.[42,43] This approach is now under evaluation in clinical trials for nAMD (NCT04514653) and diabetic retinopathy (NCT04567550).

The capsid, promoter, nature of the transgene, other *cis* regulatory factors and delivery approach all have a role in the effectiveness of transduction and transgenic expression. Thus, the effective dose threshold needs to be established for each vector, administered route, and target tissue. The increase in the expression level of AAV8-nVEGFi at the three lower doses showed a linear increasing trend; however, the nVEGFi level in eyes treated with 4×10^9 GC was approximately 1.2 times higher than that of eyes treated with 4×10^8 GC. Liu et al.[28] showed a lower expression of a high dose of AAV8-antiVEGFfab than a low dose. According to the toxicity results in this study, segmental dystrophy caused by a high AAV dose might be one of the explanations. Based on the expression assay and CNV area inhibition study, the minimum effective dose of subretinally injected AAV8-nVEGFi for nAMD treatment in mice should be in the range between 4×10^7 and 4×10^8 GC/eye. Although it is difficult to compare the effective doses from different experiments, this dose between 4×10^7 and 4×10^8 GC/eye for mice is relatively low, since the effective dose for subretinal injection in mice is typically 1×10^8 to 1×10^{10} GC/eye.[44–46] In this study, AAV8-aflibercept at 4×10^8 GC/eye performed worse than AAV8-nVEGFi at 4×10^8 GC/eye in reducing CNV areas (63.8% vs. 78.3%, $p < 0.05$), and it appeared that even AAV8-aflibercept at 4×10^9 GC/eye performed worse than AAV8-nVEGFi at 4×10^8 GC/eye (67.8% vs. 78.3%), even if the difference was not statistically significant. This is consistent with the expression results *in vivo*, where the expression of VEGF Trap in AAV8-aflibercept at 4×10^9 GC/eye was much lower than that in AAV8-nVEGFi at 4×10^8 GC/eye (1,309 ± 695.6 vs. 3,503 ± 856.9 ng/eye).

The use of AAV in the clinic demonstrated the virus's safety profile.[41] Nonetheless, it is known that AAV-mediated gene therapy of the retina can induce retinal toxicity at high doses. The nature of the transgene and the type of promoter, in addition to the AAV input dose, all have a role in determining the extent of retinal toxicity, which can be entirely avoided at low doses.[47,48] Although subretinal injection can cause traumatic retinal lesions, it tends to cause focal retinal perforation with disorganization of the ONL to complete retinal rupture.[49] Retinal thinning and retinal function impairment, observed in this study, have also been observed before in mice, dogs, and nonhuman primates and coincided with but not always limited to the region of the subretinal injection and appeared to be dose related.[47,49,50] It is unclear how AAV-mediated gene therapy triggers retinal toxicity. A direct host cell response to transgene expression or vector uptake, indirectly from harmful immune responses to the vector or the transgene product, or a combination of both are hypotheses of the mechanism.[51] High doses of AAV expressing no transgene ("null") have been shown to lead to retinal toxicity.[48] Different transgenes can cause varying degrees of damage to the retina, implying that both the capsid and the transgene play a role in toxicity.[47] In this study, we evaluated the safety of AAV8-nVEGFi, AAV8-aflibercept and AAV8-EGFP by ERG and retinal histology. The dose of each AAV appeared to be the deciding factor in the level of retinal toxicity, demonstrating that lowering the effective dose of AAV by increasing transgene

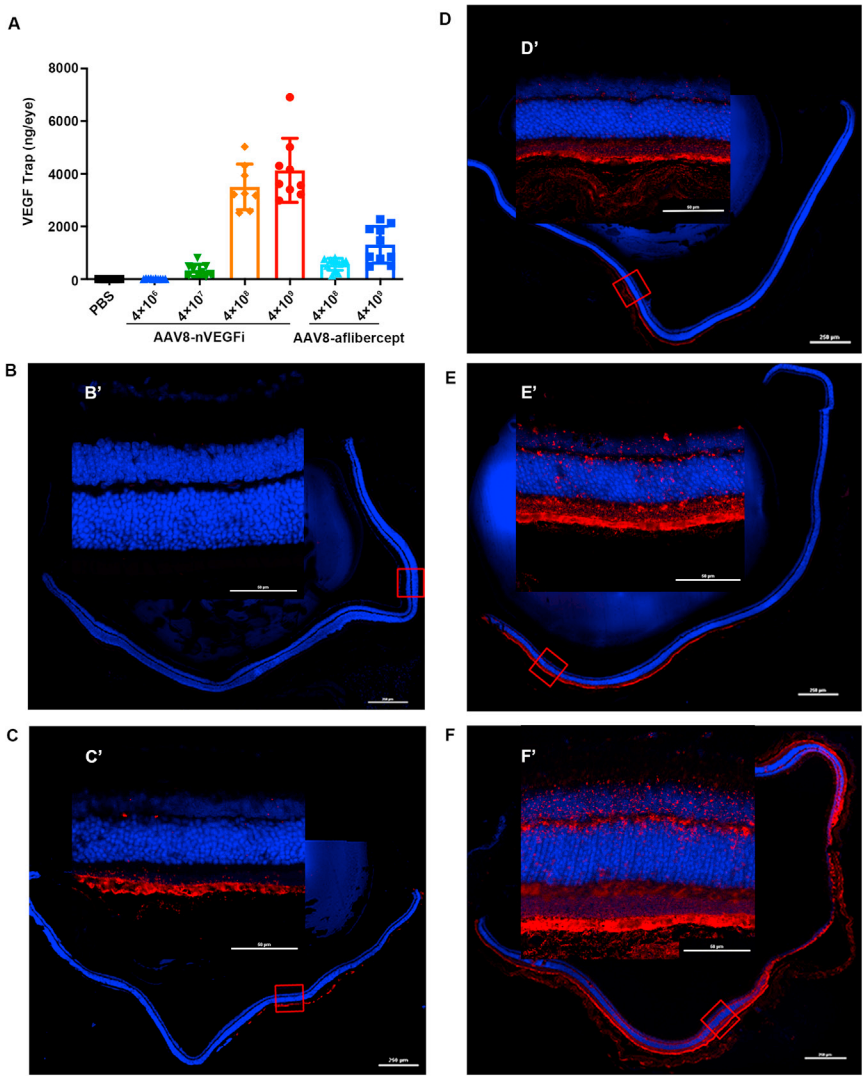

Figure 4. Expression of nVEGFi or aflibercept 12 weeks after subretinal injection of AAV8-nVEGFi or AAV8-aflibercept in mice

Twelve weeks after a single subretinal injection of PBS, AAV8-nVEGFi at 4×10^6, 4×10^7, 4×10^8, or 4×10^9 GC/eye, or AAV8-aflibercept at 4×10^8 or 4×10^9 GC/eye, the eyes of the mice were enucleated. (A) The amount of nVEGFi or aflibercept was quantified in individual eye homogenates by ELISA. Data are expressed as mean ± SD, at least n = 8 for each group. (B–F) Detection of nVEGFi mRNA in retinal sections treated with PBS or AAV8-nVEGFi by *in situ* hybridization. Magnified views of the boxed region (B′–F′) are shown. (B and B′) PBS; (C and C′) AAV8-nVEGFi at 4×10^6 GC/eye; (D and D′) AAV8-nVEGFi at 4×10^7 GC/eye; (E and E′) AAV8-nVEGFi at 4×10^8 GC/eye; (F and F′) AAV8-nVEGFi at 4×10^9 GC/eye. Scale bars, 250 μm for low power; 50 μm for high power.

expression is an efficient strategy to reduce retinal toxicity. However, the damage caused by different AAVs at the same dose differed, and AAVs encoding EGFP were more toxic with deteriorated ERG and retinal thinning, which has been reported previously.[47] Interestingly, AAV encoding aflibercept was more hazardous than AAV expressing nVEGFi according to ERG, although it had a lower expression level, implying that nVEGFi is safer for the retina than aflibercept.

In conclusion, a novel VEGF Trap, nVEGFi, was developed with a comparable capacity to bind and block VEGF *in vitro* and *in vivo*. The most notable feature of nVEGFi is its significant expression augmentation, which reduces the effective dose when delivered by AAV *in vivo* and improves the safety profile of gene therapy. The preclinical dose-escalation study demonstrated that AAV8-nVEGFi has long-term expression and can inhibit CNV safely and effectively in a mouse model.

MATERIALS AND METHODS

Plasmid construction

Aflibercept and the nVEGFi gene were codon optimized and synthesized by Genewiz, and the sequences are presented in the supplemental information. To construct the AAV vector, the codon optimized aflibercept or nVEGFi gene was subcloned into a parental *cis* plasmid containing the CB7 promoter, chicken β-actin intron, kozak sequence, and bGH polyadenylation sequence flanked by AAV2 ITRs, yielding the pAAV-aflibercept and pAAV-nVEGFi plasmid vectors, respectively. The pAAV-EGFP plasmid was constructed by replacing the nVEGFi gene of pAAV-nVEGFi with EGFP, serving as a negative control. All constructed plasmids were verified by sequencing.

VEGF traps

The nVEGFi gene was subcloned in pATX2 to construct an expression vector, pATX2-nVEGFi. One liter of HEK293F cells was transfected with pATX2-nVEGFi. Culture medium was collected on the sixth day post transfection. Then, the culture medium was pooled and filtered through a 0.22 μm membrane and loaded onto the column with Protein G resin (Smart Lifesciences). The resin was then washed with 10 column volumes of PBS (pH 7.5). The nVEGFi protein was eluted from the resin with 0.1 M glycine (pH 2.7) and neutralized with 1 M Tris-HCl (pH 8.5). The commercial anti-VEGF antibody aflibercept (Eylea, 2 mg/0.05 mL) was purchased from Bayer Pharmaceuticals.

Plasmid transfection

HEK293 cells (ATCC) were cultured with DMEM (Gibco) supplemented with 10% fetal bovine serum (FBS) (PAN Biotech) and 100 U/mL penicillin/streptomycin at 37°C with 5% CO_2. One day before transfection, HEK293 cells were seeded into 6-well plates at

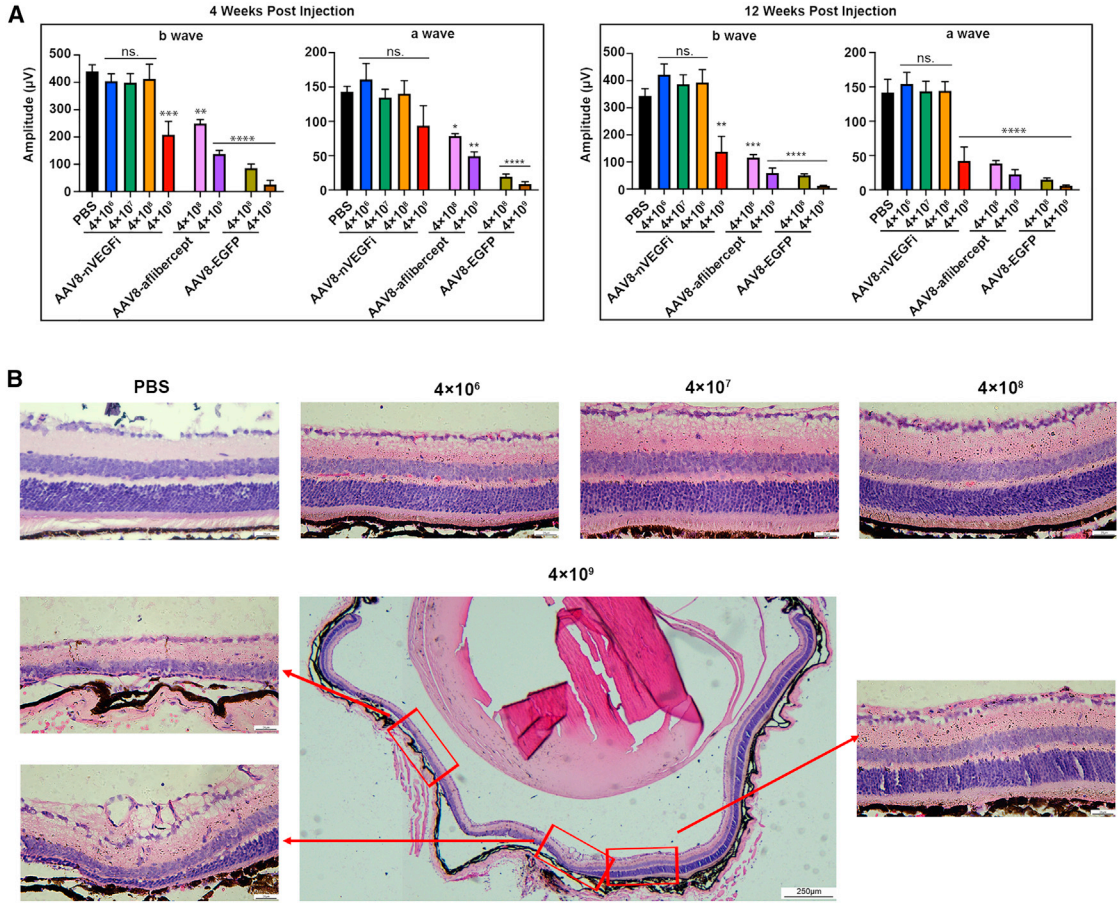

Figure 5. *In vivo* retinal toxicity evaluation of AAV8-nVEGFi

Mice were subretinally injected with PBS, AAV8-nVEGFi at 4×10^6, 4×10^7, 4×10^8, or 4×10^9 GC/eye, or AAV8-aflibercept or AAV8-EGFP at 4×10^8 or 4×10^9 GC/eye at 4 weeks old. (A) Scotopic ERG was performed at 4 and 12 weeks after injection. The b-wave and a-wave amplitudes with the stimulus at 1.2 log cd s/m^2 of each group were analyzed. Data are shown as mean ± SEM, n = 4 for PBS, n = 5 for other groups. One-way ANOVA and *post hoc* Dunnett's test were used for comparisons to the PBS control group. *$p < 0.05$, **$p < 0.01$, ***$p < 0.001$, ****$p < 0.0001$. (B) Representative photomicrographs of retinas treated with AAV8-nVEGFi 12 weeks after injection. Retinas from the PBS control, 4×10^6, 4×10^7, and 4×10^8 GC/eye dose groups showed no significant structural abnormalities (see also in Figure S3). The retina treated with 4×10^9 GC/eye showed predominant, locally extensive ONL thinning, with retinal detachment. Scale bars, 250 μm for low power; 25 μm for high power.

1×10^6 cells per well. Twenty-four hours later, cells were transfected with 360 fmol pAAV-aflibercept, pAAV-nVEGFi or pAAV-EGFP using polyethylenimine (PEI) at a 1:2 ratio of DNA:PEI in FBS-free DMEM with 100 U/mL penicillin/streptomycin. After 4 h, the medium was replaced with 1 mL FBS-free DMEM with 100 U/mL penicillin/streptomycin. For ELISA and western blot, culture medium or cells were harvested 48 h after transfection. For real-time qPCR, cells were harvested 24 h after transfection.

Real-time qPCR

Total RNA was extracted from cells with an RNAprep pure cell kit (Tiangen) according to the manufacturer's instructions. Then, RNA was reverse transcribed to cDNA using the PrimeScript RT reagent Kit with gDNA eraser (perfect real time) (Takara) according to the manufacturer's instructions. DNase was used in RNA extraction and transcription to ensure elimination of DNA contamination. Quantitative PCR was performed with TB Green Premix Ex Taq II (Takara). Primers for VEGF Trap (nVEGFi and aflibercept) and beta-actin genes are presented in the supplemental information. The qPCRs were run in triplicate for each gene per sample. The specificity of the qPCR was confirmed by detection of a single distinct peak on examination of the dissociation curve profile of the reaction product. The relative gene expression was calculated using the $\triangle\triangle$Ct method.[52] Target gene expression was normalized to the housekeeping reference gene beta-actin and then compared to the control (pAAV-aflibercept).

ELISA

Levels of VEGF-Traps in cell supernatant were measured 48 h after transfection. Levels of VEGF-Traps in eyes were measured 12 weeks after injection. Eyes were homogenized in 200 μL radioimmunoprecipitation assay buffer with a bead mill homogenizer (OMNI

international, Inc.). The concentration of nVEGFi or aflibercept was measured by ELISA using known concentrations of purified nVEGFi or aflibercept (Bayer Pharmaceuticals) to generate standard curves. Briefly, ELISA plates were coated with 100 μL human VEGF-A_{165} (1 μg/mL) in carbonate/bicarbonate buffer at 4°C overnight. Plates were washed four times with PBST (0.1% Tween in PBS) and blocked with 5% BSA in PBST for 2 h at 37°C. Plates were washed four times with PBST, and samples were added to the wells and then incubated for 2 h at 37°C. After washing four times with PBST, plates were incubated with goat anti-human IgG Fc (HRP conjugate) (Sigma-Aldrich) diluted 1:30,000 at 37°C for 1.5 h. After 4 washes with PBST, the substrate was developed with 3,3′,5,5′-tetramethyl benzidine (NeoBioscience) at room temperature (RT) for 20 min, and then 100 μL ELISA stopped solution was added (Solarbio). Plates were read by Multiskan Sky (Thermo Fisher Scientific) at 450 nm and 570 nm.

Western blot

Cell supernatants (10 μL) and lysated (20 μg) from transfected HEK293 cells were analyzed by Western blot under nonreduced or reduced conditions. Aflibercept and nVEGFi proteins were detected by anti-VEGF receptor 1 antibody (Abcam) diluted 1:2,000. Beta-actin was detected by rabbit monoclonal anti-beta actin antibody (Proteintech) diluted 1:10,000. Briefly, samples were separated by SDS-PAGE and transferred to PVDF membranes. The membranes were blocked with 5% non-fat milk in TBST at RT for 2 h and then incubated with primary antibodies at RT for 2 h. Membranes were washed three times in TBST, and HRP-conjugated goat anti-rabbit IgG (Zsbio) diluted 1:10,000 was incubated. The protein bands were visualized via Immobilon western chemiluminescent HRP substrate (Millipore). Quantification of bands was performed using ImageJ (Image Processing and Analysis in Java; the National Institutes of Health). The amount of nVEGFi in cell lysates was normalized to beta-actin.

AAV8 vector production

All AAV8 vectors were produced by triple plasmid transfection of HEK293 cells as previously described.[53] The genome titer (GC/mL) of the AAV8 vector was determined by digital droplet polymerase chain reaction (ddPCR) using forward primer 5′-TAGTTGCCAGCCATCTGTTG-3′, reverse primer 5′-TAGGAAAGGACAGTGGGAGT-3′, and probe 5′-Fam-CCCGTGCCTTCCTTGACCCT-BHQ-3′.[54] All vectors used in this study passed the endotoxin assay using the endpoint chromogenic endotoxin test kit (Xiamen Bioendo Technology Co., Ltd.).

AAV transduction *in vitro*

HEK293 cells were seeded into 96-well plates at a density of 5×10^5 cells/well in 200 μL DMEM containing 10% FBS and 100 U/mL penicillin/streptomycin. The cells were allowed to adhere for 24 h. After 24 h, cells were infected with wild-type adenovirus (H5 serotype, ATCC) at a multiplicity of infection (MOI) of 30 GC/cell. Two hours post-infection with adenovirus, cells were transduced with AAV8 vectors at an MOI of 6×10^5 GC/cell in 100 μL FBS-free DMEM with 100 U/mL penicillin/streptomycin. After 4 h, the infection medium was replaced with 100 μL DMEM containing 10% FBS and 100 U/mL penicillin/streptomycin. Three days post AAV8 infection, all the cell supernatant was collected, and the protein expression was determined by ELISA.

Surface plasmon resonance

SPR experiments were performed on a Biacore 8K (GE Healthcare) instrument using the Series S Sensor CM5 chip (GE Healthcare) at RT. The running buffer was filtered HBS-EP+ (10 mM HEPES, 150 mM NaCl, 3 mM EDTA, 0.05% polysorbate 20, pH 7.4). The surface of the CM5 chip was activated with standard amine coupling reagents, 1-ethyl-3-(3-dimethylaminopropyl) carbodiimide and N-hydroxysuccinimide. The ligands (nVEGFi and aflibercept) were diluted to 10 μg/mL with fixative reagent (10 mM sodium acetate, pH 5.0) and immobilized on the surface of a CM5 chip for 90 s. A range of concentrations of analytes (1.5625–25 nM for VEGF-A_{165} and 1.5625–50 nM for PlGF) were individually injected into the experimental channel and reference channel at a flow rate of 30 μL/min with a binding time of 120 s and a dissociation time of 600 s. The activated coupled chip surfaces were then washed with 10 mM glycine HCl, pH 1.5, to remove uncoupled residual proteins. The KD value of each antibody was calculated using analysis software.

VEGF-binding assay

The binding affinities of nVEGFi and aflibercept were measured by a human VEGF ELISA kit (Novus Biologicals) to detect residual unbound human VEGF in mixtures of nVEGFi or aflibercept (0.05–400 pM) with human VEGF-A_{165} (R&D Systems) (at a final concentration of 10 pM) and incubated at RT overnight. VEGF concentration (pM) was plotted as a function of increasing anti-VEGF molecule concentration (pM).

HUVEC proliferation assay

HUVECs (ScienCell Research Laboratories) were expanded through five passages in EGM-2 media (Lonza). HUVECs were seeded at 6×10^3 cells per well in a 96-well culture plate and incubated overnight in M199 (Gibco) starvation media (M199, 5% FBS). The following day, fresh M199 media supplemented with 20 ng/mL recombinant human VEGF-A_{165} (R&D Systems) and 1,100 pM aflibercept, nVEGFi protein or nVEGFi from the supernatant of HEK293 cells transfected with pAAV-nVEGFi were added. The concentration of nVEGFi in the supernatant of HEK293 cells transfected with pAAV-nVEGFi was measured by ELISA. HUVECs were incubated for 72 h followed by the addition of MTS reagent cell titer 96 aqueous one solution (Promega) and incubation for another 3 h. Absorbance was measured at OD490 with Multiskan Sky (Thermo Fisher Scientific).

Animals

Male C57BL/6J mice were purchased from Chengdu Dossy Experimental Animals Co., Ltd. and group-housed at four to six animals per cage in a temperature- and humidity-controlled, specific-pathogen-free animal facility at 25°C under a 12 h–12 h light–dark cycle with free access to food and water. Unless otherwise stated, mice were

anesthetized with intraperitoneal ketamine (80 mg/kg) and xylazine (12 mg/kg) in this study. The pupils were dilated with an eye drop containing 0.5% tropicamide and 0.5% phenylephrine hydrochloride. Animal experiments were approved by the Institutional Animal Care and Concern Committee at Sichuan University, and animal care was in accordance with the committee's guidelines.

Subretinal injection and intravitreal injection

Mice were subjected to bilateral, subretinal injection with AAV8-nVEGFi, AAV8-aflibercept, AAV8-EGFP, or PBS at 4 weeks of age. After anesthesia by isoflurane inhalation and pupil dilation, a limbal hole was made with a 31G needle under a stereomicroscope. Then, a blunt 33G needle (Hamilton) was inserted through the hole and directed toward the subretinal space, avoiding lens damage. Each eye was given 1 μL AAV8-nVEGFi at a titer of 4×10^6, 4×10^7, 4×10^8 or 4×10^9 GC/μL, AAV8-aflibercept or AAV8-EGFP at a titer of 4×10^8 or 4×10^9 GC/μL, or PBS. Immediately after injection, a retinal imaging microscope (Micron IV, Phoenix Research Labs) was used to observe the fundus. Injections creating subretinal blebs without massive vitreous or subretinal hemorrhage were considered to be successful. After the examination, ofloxacin eye ointment was applied to the cornea. For the aflibercept (2.5 μg, 2 μL) and nVEGFi protein (3.25 μg, 2 μL) treated groups, the mice were bilaterally intravitreally injected immediately after laser photocoagulation at 8 weeks of age. The process of intravitreal injection was similar to that of subretinal injection, except for injecting the medicine into the vitreous cavity rather than the subretinal space. All the AAV, aflibercept, and nVEGFi proteins used for intraocular injection were diluted with PBS.

Fluorescent *in situ* hybridization

Mice were euthanatized 12 weeks after injection. Eyes were enucleated and fixed in 4% paraformaldehyde (PFA)/PBS at RT for 6 h. PFA/PBS-fixed eyes were dehydrated in ethanol, cleared in xylene, and embedded in paraffin. *In situ* hybridization was performed on paraffin-embedded retinal sections using the ViewRNA ISH Tissue Assay Kit (Thermo Fisher Scientific) with a custom designed nVEGFi probe (CVX-01, assay ID: VP47VRZ, Thermo Fisher Scientific) according to the manufacturer's instructions. Briefly, paraffin sections were deparaffinized at 60°C for 4 h and washed in xylene and 100% ethanol. Tissue was incubated with 1× pretreatment solution at 95°C for 5 min, followed by protease digestion at 40°C for 20 min. Sections were fixed with 4% PFA for 5 min and incubated with alkaline phosphatase-conjugated nVEGFi probes at 40°C for 2 h. Following a 2 h incubation, sections were washed and placed in storage buffer overnight. Fluorescently labeled substrate (Fast Red) was used to detect nVEGFi probes. Slides were costained with DAPI and imaged using a confocal laser microscope (Nikon).

Laser-induced CNV

Laser induction of CNV in mice was performed by an image-guided laser system (Micron IV, Phoenix Research Laboratories) in accordance with the method described by Gong et al.[55] After anesthesia and pupil dilation, 2.5% Hypromellose was applied to the mouse cornea. The laser settings were as follows: wavelength, 532 nm; diameter, 50 μm; duration: 70 ms; and power, 260 mW. Three of four laser burns were induced around the optic disc. The distance between two laser burns and between the laser burn and the optic disc was approximately double the diameter of the optic disc. The success of the operation was confirmed by the formation of a bubble and haze area around the lesion immediately after lase photocoagulation. Eyes with significant subretinal or vitreous hemorrhage were excluded.

FFA

FFA was performed 6 days after laser photocoagulation with a retinal imaging microscope (Micron IV, Phoenix Research Laboratories). After anesthetization and pupil dilation, mice were intraperitoneally injected with 200 μL 1% fluorescein (Alcon). At 5 and 10 min after fluorescein injection, fluorescein fundus images were taken.

Immunostaining of RPE and choroidal flat-mounts

Mice were euthanized 7 days after laser photocoagulation. Eyes were enucleated and fixed in 4% PFA/PBS at RT for 1 h. RPE complexes (RPE/choroid/sclera) were prepared and permeabilized with 0.1% Triton X-100 at RT for 1 h. Then the RPE complexes were stained with 10 μg/mL IB4 (isolectin GS-IB4 from Griffonia simplicifolia, Alexa Fluor 594 conjugate, Thermo Fisher Scientific) overnight at RT. After washing with PBS 3 times, the RPE complexes were flat mounted with the scleral side down and viewed with a fluorescence microscope (DFC7000 T, Leica) at a magnification of 20×. The CNV area was measured using ImageJ (National Institutes of Health) by blind observers.

ERG

Scotopic ERG was measured 4 weeks and 12 weeks post subretinal injection. ERG was recorded under the manufacturer's instructions of the Phoenix Ganzfeld ERG (Phoenix Research Labs). Briefly, mice were dark adapted for 16 h and then all the preparations were operated under dim red light. After anesthesia, mice were placed on a heating pad to maintain body temperature. The pupils were dilated. The reference electrode was placed subcutaneously in the forehead between the ears, and the ground electrode was placed subcutaneously in the tail. A corneal electrode was placed on the cornea after applying 2.5% Hypromellose. ERG was recorded with stimulus intensity at 1.2 log cd s/m^2.

Hematoxylin and eosin

Eyes were enucleated and fixed in 4% PFA/PBS at RT for 6 h. PFA/PBS-fixed eyes were dehydrated in ethanol, cleared in xylene, and embedded in paraffin. Paraffin-embedded retinas were sectioned at 5 μm and stained with hematoxylin and eosin according to standard protocols for light microscopy and photomicrography (Leica).

Statistical analysis

Data are presented as mean ± SD in Figures 1, 2 and 4, as median (P25, P75) in Figure 3, and as mean ± SEM in Figure 5. GraphPad Prism (University of California, San Diego, California) was used to perform statistical analysis and make figures. Comparisons were

considered statistically significant when $p < 0.05$. The Student *t* test was used to analyze the difference between two groups in Figure 1. One-way ANOVA analysis with Tukey's *post hoc* test was used in Figures 2B and 4A. The nonparametric Kruskal-Wallis with *post hoc* Dunnett's test were used to analyze the differences in CNV area among different groups in Figure 3E. The comparison of ERG among different groups in Figure 5A was carried out by one-way ANOVA and *post hoc* Dunnett's test.

SUPPLEMENTAL INFORMATION

Supplemental information can be found online at https://doi.org/10.1016/j.omtm.2022.01.002.

ACKNOWLEDGMENTS

This work was supported by the Joint Funds of the National Natural Science Foundation of China (grant no. U19A2002), National Major Scientific and Technological Special Project for "Significant New Drugs Development" (no. 2018ZX09733001-005-002), and the Science and Technology Major Project of Sichuan Province (no. 2017SZDZX0011).

AUTHOR CONTRIBUTIONS

Y.Y., F.L., and Y.W. conceived this study and designed the experiments; K.S. and J.S. constructed the plasmid vectors and conducted the *in vitro* studies; K.S., J.S., Q.W., and Y.L. performed mouse studies; X.J. produced AAV8 vector; Q.W. performed real-time qPCR; J.X. performed ddPCR and endotoxin assays; K.S., X.Z., Q.Z., and R.L. conducted immunostaining, *in situ* hybridization and hematoxylin and eosin studies; K.S. wrote the manuscript; Y.Y., H.D., and F.L. edited the manuscript, and all authors read and approved the final manuscript.

DECLARATION OF INTERESTS

The authors declare no competing interests.

REFERENCES

1. Mitchell, P., Liew, G., Gopinath, B., and Wong, T. (2018). Age-related macular degeneration. Lancet *392*, 1147–1159.
2. Wong, W.L., Su, X., Li, X., Cheung, C.M., Klein, R., Cheng, C.Y., and Wong, T.Y. (2014). Global prevalence of age-related macular degeneration and disease burden projection for 2020 and 2040: a systematic review and meta-analysis. Lancet Glob. Health *2*, e106–e116.
3. Lopez, P.F., Sippy, B.D., Lambert, H.M., Thach, A.B., and Hinton, D.R. (1996). Transdifferentiated retinal pigment epithelial cells are immunoreactive for vascular endothelial growth factor in surgically excised age-related macular degeneration-related choroidal neovascular membranes. Invest Ophthalmol. Vis. Sci. *37*, 855–868.
4. Macular Photocoagulation Study Group (1982). Argon laser photocoagulation for senile macular degeneration. Results of a randomized clinical trial. Arch. Ophthalmol. *100*, 912–918.
5. Schlötzer-Schrehardt, U., Viestenz, A., Naumann, G., Laqua, H., Michels, S., and Schmidt-Erfurth, U. (2002). Dose-related structural effects of photodynamic therapy on choroidal and retinal structures of human eyes. Graefe's Arch. Clin. Exp. Ophthalmol. *240*, 748–757.
6. Falavarjani, K., and Nguyen, Q. (2013). Adverse events and complications associated with intravitreal injection of anti-VEGF agents: a review of literature. Eye *27*, 787–794.
7. Kim, L., Mehta, H., Barthelmes, D., Nguyen, V., and Gillies, M. (2016). Metaanalysis of real-world outcomes of intravitreal ranibizumab for the treatment of neovascular age-related macular degeneration. Retina *36*, 1418–1431.
8. Khanani, A.M. (2021). ADVM-022 intravitreal gene therapy for neovascular AMD - phase 1 OPTIC study at retina society. https://adverum.com/wp-content/uploads/2021/10/OPTIC-Retina-Society-Meeting-Updated-9-30-2021a.pdf.
9. REGENXBIO (2019). REGENXBIO announces additional positive interim phase I/IIa trial update for RGX-134 for the treatment of wet AMD at the American Academy of ophthalmology 2019 annual meeting. https://www.prnewswire.com/news-releases/regenxbio-announces-additional-positive-interim-phase-iiia-trial-update-for-rgx-314-for-the-treatment-of-wet-amd-at-the-american-academy-of-ophthalmology-2019-annual-meeting-300937385.html.
10. Cashman, S.M., Bowman, L., Christofferson, J., and Kumar-Singh, R. (2006). Inhibition of choroidal neovascularization by adenovirus-mediated delivery of short hairpin RNAs targeting VEGF as a potential therapy for AMD. Invest Ophthalmol. Vis. Sci. *47*, 3496–3504.
11. Askou, A.L., Pournaras, J.A., Pihlmann, M., Svalgaard, J.D., Arsenijevic, Y., Kostic, C., Bek, T., Dagnaes-Hansen, F., Mikkelsen, J.G., Jensen, T.G., et al. (2012). Reduction of choroidal neovascularization in mice by adeno-associated virus-delivered anti-vascular endothelial growth factor short hairpin RNA. J. Gene Med. *14*, 632–641.
12. Askou, A.L., Benckendorff, J.N.E., Holmgaard, A., Storm, T., Aagaard, L., Bek, T., Mikkelsen, J.G., and Corydon, T.J. (2017). Suppression of choroidal neovascularization in mice by subretinal delivery of multigenic lentiviral vectors encoding anti-angiogenic MicroRNAs. Hum. Gene Ther. Methods *28*, 222–233.
13. Lin, F.L., Wang, P.Y., Chuang, Y.F., Wang, J.H., Wong, V.H.Y., Bui, B.V., and Liu, G.S. (2020). Gene therapy intervention in neovascular eye disease: a recent update. Mol. Ther. *28*, 2120–2138.
14. Campochiaro, P., Nguyen, Q., Shah, S., Klein, M., Holz, E., Frank, R., Saperstein, D., Gupta, A., Stout, J., Macko, J., et al. (2006). Adenoviral vector-delivered pigment epithelium-derived factor for neovascular age-related macular degeneration: results of a phase I clinical trial. Hum. Gene Ther. *17*, 167–176.
15. Rakoczy, E., Lai, C., Magno, A., Wikstrom, M., French, M., Pierce, C., Schwartz, S., Blumenkranz, M., Chalberg, T., Degli-Esposti, M., et al. (2015). Gene therapy with recombinant adeno-associated vectors for neovascular age-related macular degeneration: 1 year follow-up of a phase 1 randomised clinical trial. Lancet *386*, 2395–2403.
16. Campochiaro, P.A., Lauer, A.K., Sohn, E.H., Mir, T.A., Naylor, S., Anderton, M.C., Kelleher, M., Harrop, R., Ellis, S., and Mitrophanous, K.A. (2017). Lentiviral vector gene transfer of endostatin/angiostatin for macular degeneration (GEM) study. Hum. Gene Ther. *28*, 99–111.
17. Maclachlan, T.K., Lukason, M., Collins, M., Munger, R., Isenberger, E., Rogers, C., Malatos, S., Dufresne, E., Morris, J., Calcedo, R., et al. (2011). Preclinical safety evaluation of AAV2-sFLT01- a gene therapy for age-related macular degeneration. Mol. Ther. *19*, 326–334.
18. Heier, J., Kherani, S., Desai, S., Dugel, P., Kaushal, S., Cheng, S., Delacono, C., Purvis, A., Richards, S., Le-Halpere, A., et al. (2017). Intravitreous injection of AAV2-sFLT01 in patients with advanced neovascular age-related macular degeneration: a phase 1, open-label trial. Lancet *390*, 50–61.
19. ADVERUM (2021). Adverum provides update on ADVM-022 and the INFINITY trial in patients with diabetic macular edema. https://investors.adverum.com/news/news-details/2021/Adverum-Provides-Update-on-ADVM-022-and-the-INFINITY-Trial-in-Patients-with-Diabetic-Macular-Edema/default.aspx.
20. Ong, T., Pennesi, M.E., Birch, D.G., Lam, B.L., and Tsang, S.H. (2019). Adeno-associated viral gene therapy for inherited retinal disease. Pharm. Res. *36*, 34.
21. Vandenberghe, L.H., Bell, P., Maguire, A.M., Cearley, C.N., Xiao, R., Calcedo, R., Wang, L., Castle, M.J., Maguire, A.C., Grant, R., et al. (2011). Dosage thresholds for AAV2 and AAV8 photoreceptor gene therapy in monkey. Sci. Transl. Med. *3*, 88ra54.
22. Holash, J., Davis, S., Papadopoulos, N., Croll, S., Ho, L., Russell, M., Boland, P., Leidich, R., Hylton, D., Burova, E., et al. (2002). VEGF-Trap: a VEGF blocker with potent antitumor effects. Proc. Natl. Acad. Sci. U S A *99*, 11393–11398.
23. Cao, Y. (2009). Positive and negative modulation of angiogenesis by VEGFR1 ligands. Sci. Signal. *2*, 1–11.

24. Davis-Smyth, T., Chen, H., Park, J., Presta, L.G., and Ferrara, N. (1996). The second immunoglobulin-like domain of the VEGF tyrosine kinase receptor Flt-1 determines ligand binding and may initiate a signal transduction cascade. Embo j *15*, 4919–4927.

25. Herley, M., Yu, Y., Whitney, R., and Sato, J. (1999). Characterization of the VEGF binding site on the Flt-1 receptor. Biochem. Biophys. Res. Commun. *262*, 731–738.

26. Lee, J.E., Kim, C., Yang, H., Park, I., Oh, N., Hua, S., Jeong, H., An, H.J., Kim, S.C., Lee, G.M., et al. (2015). Novel glycosylated VEGF decoy receptor fusion protein, VEGF-Grab, efficiently suppresses tumor angiogenesis and progression. Mol. Cancer Ther. *14*, 470–479.

27. Buck, T.M., and Wijnholds, J. (2020). Recombinant adeno-associated viral vectors (rAAV)-vector elements in ocular gene therapy clinical trials and transgene expression and bioactivity assays. Int. J. Mol. Sci. *21*, 4197.

28. Liu, Y., Fortmann, S.D., Shen, J., Wielechowski, E., Tretiakova, A., Yoo, S., Kozarsky, K., Wang, J., Wilson, J.M., and Campochiaro, P.A. (2018). AAV8-antiVEGFfab ocular gene transfer for neovascular age-related macular degeneration. Mol. Ther. *26*, 542–549.

29. Grishanin, R., Vuillemenot, B., Sharma, P., Keravala, A., Greengard, J., Gelfman, C., Blumenkrantz, M., Lawrence, M., Hu, W., Kiss, S., et al. (2019). Preclinical evaluation of ADVM-022, a novel gene therapy approach to treating wet age-related macular degeneration. Mol. Ther. *27*, 118–129.

30. Askou, A.L., Aagaard, L., Kostic, C., Arsenijevic, Y., Hollensen, A.K., Bek, T., Jensen, T.G., Mikkelsen, J.G., and Corydon, T.J. (2015). Multigenic lentiviral vectors for combined and tissue-specific expression of miRNA- and protein-based antiangiogenic factors. Mol. Ther. Methods Clin. Dev. *2*, 14064.

31. Biswal, M.R., Prentice, H.M., Smith, G.W., Zhu, P., Tong, Y., Dorey, C.K., Lewin, A.S., and Blanks, J.C. (2018). Cell-specific gene therapy driven by an optimized hypoxia-regulated vector reduces choroidal neovascularization. J. Mol. Med. *96*, 1107–1118.

32. Askou, A., and Corydon, T. (2018). Development of multigenic lentiviral vectors for cell-specific expression of antiangiogenic miRNAs and protein factors. Methods Mol. Biol. *1715*, 47–60.

33. Reid, C.A., Nettesheim, E.R., Connor, T.B., and Lipinski, D.M. (2018). Development of an inducible anti-VEGF rAAV gene therapy strategy for the treatment of wet AMD. Sci. Rep. *8*, 11763.

34. Holmgaard, A., Askou, A., Benckendorff, J., Thomsen, E., Cai, Y., Bek, T., Mikkelsen, J., and Corydon, T. (2017). In vivo knockout of the vegfa gene by lentiviral delivery of CRISPR/Cas9 in mouse retinal pigment epithelium cells. molecular therapy. Nucleic Acids *9*, 89–99.

35. Kim, E., Koo, T., Park, S.W., Kim, D., Kim, K., Cho, H.Y., Song, D.W., Lee, K.J., Jung, M.H., Kim, S., et al. (2017). In vivo genome editing with a small Cas9 orthologue derived from *Campylobacter jejuni*. Nat. Commun. *8*, 14500.

36. Kim, K., Park, S.W., Kim, J.H., Lee, S.H., Kim, D., Koo, T., Kim, K.E., Kim, J.H., and Kim, J.S. (2017). Genome surgery using Cas9 ribonucleoproteins for the treatment of age-related macular degeneration. Genome Res. *27*, 419–426.

37. Koo, T., Park, S.W., Jo, D.H., Kim, D., Kim, J.H., Cho, H.-Y., Kim, J., Kim, J.H., and Kim, J.-S. (2018). CRISPR-LbCpf1 prevents choroidal neovascularization in a mouse model of age-related macular degeneration. Nat. Commun. *9*, 1855.

38. Seitz, I.P., Michalakis, S., Wilhelm, B., Reichel, F.F., Ochakovski, G.A., Zrenner, E., Ueffing, M., Biel, M., Wissinger, B., Bartz-Schmidt, K.U., et al. (2017). Superior retinal gene transfer and biodistribution profile of subretinal versus intravitreal delivery of AAV8 in nonhuman primates. Invest. Ophthalmol. Vis. Sci. *58*, 5792–5801.

39. Dias, M.S., Araujo, V.G., Vasconcelos, T., Li, Q., Hauswirth, W.W., Linden, R., and Petrs-Silva, H. (2019). Retina transduction by rAAV2 after intravitreal injection: comparison between mouse and rat. Gene Ther. *26*, 479–490.

40. Kotterman, M., Yin, L., Strazzeri, J., Flannery, J., Merigan, W., and Schaffer, D. (2015). Antibody neutralization poses a barrier to intravitreal adeno-associated viral vector gene delivery to non-human primates. Gene Ther. *22*, 116–126.

41. Russell, S., Bennett, J., Wellman, J.A., Chung, D.C., Yu, Z.F., Tillman, A., Wittes, J., Pappas, J., Elci, O., McCague, S., et al. (2017). Efficacy and safety of voretigene neparvovec (AAV2-hRPE65v2) in patients with RPE65-mediated inherited retinal dystrophy: a randomised, controlled, open-label, phase 3 trial. Lancet *390*, 849–860.

42. Yiu, G., Chung, S.H., Mollhoff, I.N., Nguyen, U.T., Thomasy, S.M., Yoo, J., Taraborelli, D., and Noronha, G. (2020). Suprachoroidal and subretinal injections of AAV using transscleral microneedles for retinal gene delivery in nonhuman primates. Mol. Ther. Methods Clin. Dev. *16*, 179–191.

43. Ding, K., Shen, J., Hafiz, Z., Hackett, S.F., Silva, R.L.E., Khan, M., Lorenc, V.E., Chen, D., Chadha, R., Zhang, M., et al. (2019). AAV8-vectored suprachoroidal gene transfer produces widespread ocular transgene expression. J. Clin. Invest. *129*, 4901–4911.

44. Ye, G.J., Budzynski, E., Sonnentag, P., Nork, T.M., Sheibani, N., Gurel, Z., Boye, S.L., Peterson, J.J., Boye, S.E., Hauswirth, W.W., et al. (2016). Cone-specific promoters for gene therapy of achromatopsia and other retinal diseases. Hum. Gene Ther. *27*, 72–82.

45. Dinculescu, A., Stupay, R.M., Deng, W.T., Dyka, F.M., Min, S.H., Boye, S.L., Chiodo, V.A., Abrahan, C.E., Zhu, P., Li, Q., et al. (2016). AAV-mediated clarin-1 expression in the mouse retina: implications for USH3A gene therapy. PLoS ONE *11*, e0148874.

46. Hori, T., Fukutome, M., Maejima, C., Matsushima, H., Kobayashi, K., Kitazawa, S., Kitahara, R., Kitano, K., Kobayashi, K., Moritoh, S., et al. (2019). Gene delivery to cone photoreceptors by subretinal injection of rAAV2/6 in the mouse retina. Biochem. Biophys. Res. Commun. *515*, 222–227.

47. Khabou, H., Cordeau, C., Pacot, L., Fisson, S., and Dalkara, D. (2018). Dosage thresholds and influence of transgene cassette in adeno-associated virus-related toxicity. Hum. Gene Ther. *29*, 1235–1241.

48. Xiong, W., Wu, D.M., Xue, Y., Wang, S.K., Chung, M.J., Ji, X., Rana, P., Zhao, S.R., Mai, S., and Cepko, C.L. (2019). AAV cis-regulatory sequences are correlated with ocular toxicity. Proc. Natl. Acad. Sci. U S A *116*, 5785–5794.

49. Jacobson, S.G., Acland, G.M., Aguirre, G.D., Aleman, T.S., Schwartz, S.B., Cideciyan, A.V., Zeiss, C.J., Komaromy, A.M., Kaushal, S., Roman, A.J., et al. (2006). Safety of recombinant adeno-associated virus type 2-RPE65 vector delivered by ocular subretinal injection. Mol. Ther. *13*, 1074–1084.

50. MacLachlan, T.K., Milton, M.N., Turner, O., Tukov, F., Choi, V.W., Penraat, J., Delmotte, M.H., Michaut, L., Jaffee, B.D., and Bigelow, C.E. (2018). Nonclinical safety evaluation of scAAV8-RLBP1 for treatment of RLBP1 retinitis pigmentosa. Mol. Ther. Methods Clin. Dev. *8*, 105–120.

51. Bucher, K., Rodríguez-Bocanegra, E., Dauletbekov, D., and Fischer, M.D. (2020). Immune responses to retinal gene therapy using adeno-associated viral vectors - implications for treatment success and safety. Prog. Retin. Eye Res. *83*, 100915.

52. Pfaffl, M.W. (2001). A new mathematical model for relative quantification in real-time RT-PCR. Nucleic Acids Res. *29*, e45.

53. Lock, M., Alvira, M., Vandenberghe, L.H., Samanta, A., Toelen, J., Debyser, Z., and Wilson, J.M. (2010). Rapid, simple, and versatile manufacturing of recombinant adeno-associated viral vectors at scale. Hum. Gene Ther. *21*, 1259–1271.

54. Lock, M., Alvira, M.R., Chen, S.J., and Wilson, J.M. (2014). Absolute determination of single-stranded and self-complementary adeno-associated viral vector genome titers by droplet digital PCR. Hum. Gene Ther. Methods *25*, 115–125.

55. Gong, Y., Li, J., Sun, Y., Fu, Z., Liu, C., Evans, L., Tian, K., Saba, N., Fredrick, T., Morss, P., et al. (2015). Optimization of an image-guided laser-induced choroidal neovascularization model in mice. PLoS One *10*, e0132643.